Eur. Phys. J. B **9**, 739–753 (1999)

THE EUROPEAN PHYSICAL JOURNAL B

EDP Sciences

Can one hear the shape of an electrode? I. Numerical study of the active zone in Laplacian transfer

B. Sapoval[1,a], M. Filoche[1,b], K. Karamanos[1], and R. Brizzi[2]

[1] Laboratoire de Physique de la Matière Condensée, École Polytechnique, 91128 Palaiseau Cedex, France
[2] Centre de Mathématiques Appliquées, École Polytechnique, 91128 Palaiseau Cedex, France

Received 3 November 1998 and Received in final form 8 December 1998

Abstract. The concept of active zone in the Laplacian transport to and across irregular interfaces is rigorously introduced. It applies to arbitrary geometries and uses the coarse-graining method proposed by Sapoval to compute the flux across an irregular interface from its geometry without solving the general Laplace problem. Such transport play a dominant role in electrochemistry, heterogeneous catalysis and physiological diffusion processes. In the field of electrochemistry, the method permits one to predict the impedance of an electrode of arbitrary geometry for any value of the frequency. It shows that, for systems with aspect ratios of the order of a few times unity or less, impedance spectroscopy yields in principle a reliable approximate measure of the length of the chord corresponding to a perimeter length inversely proportional to the interface capacitance and frequency. For these cases, impedance spectroscopy can determine the shape of an electrode to the extent that the knowledge of the average chord length as a function of the perimeter determines the shape. For systems of arbitrary geometry, it is shown that impedance spectroscopy permits a measure of the size of the active zone. These results can be transposed to several problems related to Laplacian transfer, such as etching of irregular solids and catalysis in the Eley-Rideal regime.

PACS. 82.80.Fk Electrochemical methods – 64.60.Ak Renormalization-group, fractal, and percolation studies of phase transitions – 82.65.Jv Heterogeneous catalysis at surfaces

1 Introduction

The title of this paper refers to a celebrated work by Mark Kac "Can one hear the shape of a drum?" which has triggered many studies about the eigenvalue distribution for the harmonic equation [1]. The answer to that question was shown to be negative since drums of different shapes may have the same spectrum [2].

In the work presented here and in the following paper [3], two very different answers to the question addressed in the title are given. In both cases, the question is transformed in a purely mathematical problem. However, the formal nature of these two problems, that will be called **problem I** and **problem II**, are essentially different.

Here we discuss how electrode impedance spectroscopy permits one to measure in all cases the length of the active zone in an electrodic process, that is the length of the zone where the transfer of charge or matter or excitation due to Laplacian transport is really effective. For the class of geometries which do not contain deep pores with large aspect ratios, it is shown that one can answer positively, although approximately, the question. More precisely we show that, at least in $d = 2$, impedance spectroscopy gives a reliable measure of the average chord length corresponding to a perimeter which is a simple function of the frequency. This paper is restricted to the introduction and to the critical tests of these notions. Detailed demonstrations of some of the notions that are used here are presented in the following paper [3].

We consider the linear transport across irregular interfaces such as electrodes or membranes, a common phenomenon in many natural or industrial processes. The basic concepts used here are the general properties of fields deriving from Laplacian potentials. They can then be applied to any transport due to Laplacian fields. Examples are the electrical response of electrodes in contact with electrolytes or diffusional steady states transport to and across a membrane where neutral reacting species are brought to the surface by diffusion currents instead of electrical currents in electrochemical systems [4]. For instance, it applies to the diffusional transport of oxygen in the terminal part of the respiratory system of mammals [5]. Its frequent occurrence and its practical importance have justified a number of studies on the influence of the interface geometry on the net flux across such interfaces. The possible role of the fractal structure of the interface has been extensively studied. (For a review on fractal

[a] e-mail: bernard.sapoval@polytechnique.fr
[b] e-mail: marcel.filoche@polytechnique.fr

electrodes, see references [6,7] and the references therein). The same problem arises in the Eley-Rideal mechanism in heterogeneous catalysis where reactants have to diffuse to a catalytic porous surface in order to react [8]. In a still different situation, the same phenomena may play a role in nuclear magnetic relaxation of a fluid embedded into a porous material. In that last situation, nuclear spins diffuse with molecular diffusion towards pore walls which may have magnetic relaxing properties [9,10].

The purpose of this paper is to introduce rigorously and to test the notion of active zone from the notion of surface dissipation. As the physical dissipation in an interface cannot be measured directly, it is of interest to compare this dissipation, or more precisely the "heat impedance" to be defined, to the quantity that is currently measured by impedance spectroscopy. The comparison will be made for simple irregular cases, for a standard fractal electrode, and for deep irregular pores.

Recently, a finite scale renormalization procedure has been proposed which, as shown here, is a method to estimate the size of the active zone. This method should permit one to compute the response of any structure in $d = 2$ from the geometry only of the interface (or from its picture) [11]. This method has been called the "rope walk" method in [8]. It is called here the "land surveyor method" because it is based on a finite size renormalization of the real topography of the electrode. Finally, we address the inverse problem: "to what extent can the shape of the electrode be found from the knowledge of the frequency dependence of the impedance?". The answer that is given to that question, although approximate, is positive in the case where the aspect ratio is not too large. It is also shown that impedance spectroscopy makes possible the detection of deep pores.

The notion of active zone is first introduced, and its connection with the "land surveyor method" discussed. Here, we will eventually use some exact theoretical results which are obtained in the following paper. Next, the prediction of the method is tested by extended numerical simulations. The following section is devoted to the discussion of the inverse problem: Can one here the shape of an electrode? And finally, the practical consequences of this work are discussed.

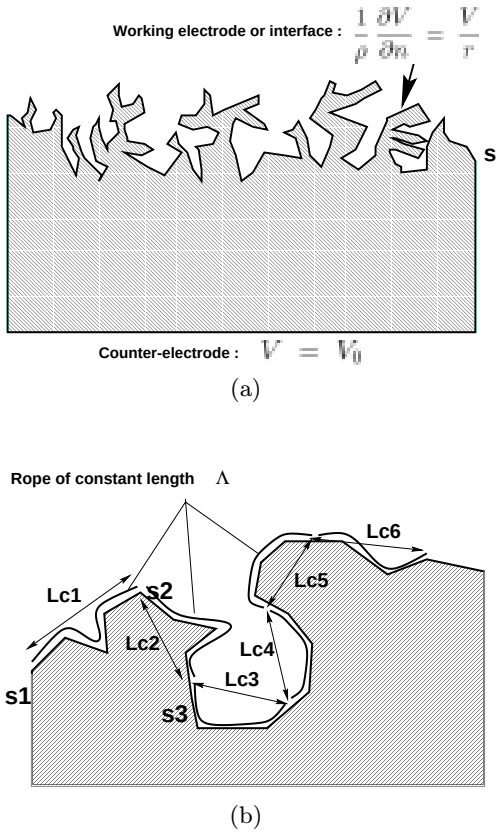

Fig. 1. General Overview. (a) Schematic representation of the type of electrochemical cell under study. The working electrode presents an irregular geometry. The electric potential obeys Laplace equation in the bulk. A constant potential V_0 is applied on the counter electrode. The finite transfer across the working interface imposes a mixed boundary condition $V/\nabla V = r/\rho = \Lambda$. In the equivalent steady state diffusion problem, a concentration C_0 is maintained on the diffusion source situated at the counter electrode location. The boundary condition in that case is $C/\nabla C = W/D = \Lambda$. (b) Scheme of the coarse-graining or finite renormalization procedure. Successive ropes of length Λ determine successive chords of lengths L_{c1}, L_{c2},...

2 The notion of active zone

We first recall briefly the nature of the problem that we address. Consider the electrochemical cell shown in Figure 1a: the response of this cell is governed by the resistivity ρ of the electrolyte and by the rate of charge transfer occurring at the interface. The transport equation in the volume is $\mathbf{J} = -\nabla V/\rho$, where $\mathbf{J}$ is the vector current in the electrolyte and the potential V obeys the Laplace equation $\Delta V = 0$ in the bulk of the electrolyte.

The rate of charge transfer occurring at the interface is characterized by a resistance per unit surface r (known as the faradaic resistance) and if any, by a capacitance γ per unit surface. The current at the surface is $\mathbf{J}_n = -V(r^{-1} + j\gamma\omega)$, where V is the local potential in the electrolyte at some point "very near" the interface. We restrict our study to the case where the smallest geometrical feature in the geometry is much larger than the Debye length. Consequently, in the region that we consider, we may use the Laplace equation instead of the Poisson equation for the electrical potential [12,13]. There is then a single parameter $(r^{-1} + j\gamma\omega)$ to describe the charge transfer at the interface, and the extension from d.c. to a.c., or inversely will be discussed later. We here consider only the d.c. problem as illustrated in Figure 1a where the outer electrode is at potential V_0 and the inner electrode at the zero potential. Due to charge conservation, the current $\mathbf{J}_n = -V/r$ crossing the electrode surface must be equal to the Ohmic current $\mathbf{J}_n = -\nabla_n V/\rho$ reaching from the bulk. As a consequence the boundary condition can be

written as

$$\frac{V}{\nabla_{\rm n} V} = \Lambda = \frac{r}{\rho} \cdot \tag{1}$$

This introduces a finite length scale Λ in the problem. From a mathematical point of view, the problem is to find the properties of the Laplacian field on the surface with the so-called Fourier or mixed boundary condition (1). The role of the length Λ on the current distribution on irregular electrodes was already recognized in the late forties [14,15].

There exist two ways to define the electrode impedance. First, the electrode impedance can be defined by the way it is measured through impedance spectroscopy. In this frame, the equivalent circuit of a cell like that of Figure 1 is represented by two resistances in series. First, the resistance of the electrolyte R_0 which is proportional to the electrolyte resistivity ρ and depends upon the geometry of the cell. It is the value of the cell impedance $Z_{\rm cell}$ for $r = 0$. Second, the electrode resistance $Z_{\rm ode,spect.}$ which depends on r, ρ and the electrode geometry, such that

$$Z_{\rm cell,spect.} = R_0 + Z_{\rm ode,spect.}. \tag{2}$$

We introduce an other definition of the electrode impedance from the power heating at the electrode interface. We call that impedance $Z_{\rm ode,heat}$. It is defined by the relation

$$Z_{\rm ode,heat}\ I^2 = \int_{\rm electrode} [r j_{\rm n}^2]\ {\rm d}A \tag{3}$$

where the integral is taken over the electrode surface. These two impedances need not be identical. The interest of the second definition is that it describes directly the electrode impedance in terms of the real surface resistance r which is "heated" by the local current $j_{\rm n}$. In this frame, the boundary condition (1) determines the distribution of $j_{\rm n}$. In order to obtain quantities which can be compared to measurements made on real electrochemical cells [7], we introduce the thickness b of the cell along the third dimension such that ${\rm d}A = b \times {\rm d}s$, where s is the curvilinear coordinate along the electrode. Now $Z_{\rm ode,heat}$ can be written

$$Z_{\rm ode,heat} = \int_{\rm electrode} rb \left(\frac{j_{\rm n}}{I}\right)^2\ {\rm d}s. \tag{4}$$

The total current I is the integral of the current density $I = \int_{\rm electrode} j_{\rm n} b {\rm d}s$. Using a normalized current density $j_{\rm n,N} = j_{\rm n} b / I$ normalized in the plane by

$$\int_{\rm electrode} j_{\rm n,N}\ {\rm d}s = 1 \tag{5}$$

we have

$$Z_{\rm ode,heat} = \frac{r}{b} \int_{\rm electrode} (j_{\rm n,N})^2 {\rm d}s. \tag{6}$$

This definition allows one to introduces naturally a "length of the active zone" by

$$L_{\rm act.,heat} = \left[\int_{\rm electrode} j_{\rm n,N}^2 {\rm d}s\right]^{-1} \tag{7}$$

from which the heat impedance takes the ordinary form

$$Z_{\rm ode,heat} = \frac{r}{b L_{\rm act.,heat}} \cdot \tag{8}$$

It should be stressed that in general, the "spectroscopic" impedance $Z_{\rm ode,spect.}$ and the "heat" impedance $Z_{\rm ode,heat}$ are different because the power $I^2 Z_{\rm ode,spect.}$ is equal to $I^2 Z_{\rm cell} - I^2 R_0$. This is the difference of the power dissipated in the cell for finite r minus the power dissipated in the electrolyte when $r = 0$. On the opposite, $Z_{\rm ode,heat}$ measures the power really dissipated in the interface. As shown later from theory and from numerical simulation, both quantities are close, so that the spectroscopic impedance can be considered as an approximate measure of the length of the active zone $L_{\rm act.,heat}$. Moreover, it will be shown rigorously in the following paper that, whatever the electrode geometry, the following relation holds:

$$Z_{\rm ode,heat} = r\ \frac{\partial Z_{\rm ode,spect.}}{\partial r} \cdot \tag{9}$$

It should be stressed that the heat impedance is not the real part of the electrode impedance measured in spectroscopy. This will be discussed later.

The knowledge of the experimental quantity $Z_{\rm ode,spect.}$ permits then, in principle, the computation of $Z_{\rm ode,heat}$ and of the length of the active zone. The goal of our investigation is first to compute and discuss the electrode impedance in approximate but simple "topographic" terms. In a second step we discuss the inverse problem which can be formulated as follows: when ones measures the impedance of an irregular electrode, what can be learned about its geometry?

There are in fact two cases. First, consider surfaces with not too large aspect ratios. It will be shown that in this case the "land surveyor method" allows to transform the inverse physical problem in a purely mathematical problem. Second, whatever the geometry, the impedance spectra really measures the length of the active zone through relations (8) and (9). As we will see in the following discussion, it makes possible the detection of deep pores.

3 The land surveyor method

The Land Surveyor Method (LSM) permits one in principle to compute $Z_{\rm ode}$ directly from the electrode shape and

the value of Λ [11]. The idea is to substitute the problem of Laplacian transfer across a real electrode (which presents a finite transfer rate) by a problem of Laplacian field obeying the Dirichlet boundary condition ($V = 0$) but with a different geometry, obtained by a coarse-graining of the real geometry to a physical scale determined by the length Λ.

The Dirichlet Laplace problem on irregular electrodes has been thoroughly studied, at least in $d = 2$. Note that the Dirichlet problem is known as that of "primary current distribution" in the field of electrochemistry. More specifically, an important theorem, Makarov's theorem, describing the properties of the current distribution on an irregular (possibly fractal) electrode can be used [16,17]. This theorem states that the information dimension of the harmonic measure (here the harmonic measure is the normalized current density) on a singly connected electrode in $d = 2$ is exactly equal to 1. This very special property of the Laplacian field can be illustrated in the following manner: whatever the shape of the working electrode, the size of the region where most of the current flows is proportional to the overall size (or diameter) L of the electrode under a dilation transformation.

This result generalizes to arbitrary geometry a fact which has been known for a long time for simple geometries. It has a simple but profound meaning in terms of the screening efficiency of the geometrical irregularity, and this is what we use here. We consider the simplest description of an irregular electrode: the ratio $S = L_{\rm p}/L$ of the perimeter length $L_{\rm p}$ divided by its size or diameter L [18]. This number S, although defined very simply, has a direct physical significance. It measures the screening efficiency of the irregularity of the structure for Dirichlet Laplacian fields for the following reason. Whatever the geometry, if the active zone has a size L, then as

$$L = \frac{L_{\rm p}}{S}, \tag{10}$$

the factor $1/S$ can be considered to be the "screening efficiency" of the primary current distribution due to the geometrical irregularity. This is the physical significance of Makarov's theorem.

This result cannot be applied as such to an electrochemical cell because the boundary condition on the electrode is not $V = 0$ but $V/\nabla_{\rm n} V = \Lambda$. We are then in the situation known as the secondary current distribution in electrochemistry. The real boundary condition introduces the physical scale Λ in the problem. The procedure that was proposed in [11] is to switch from the real geometry obeying the real boundary condition to a coarse-grained geometry obeying the Dirichlet boundary condition, with the coarse-graining depending on Λ. In a second step, one can use the screening efficiency of the coarse-grained geometry to find the active zone, hence its impedance.

This procedure has been recently applied to the study of inhomogeneous irregular electrodes [19], and we recall here its essential ingredients. The curvilinear coordinate along the electrode is called s. A region of perimeter $\mathrm{d}s$ around the curvilinear coordinate s presents an elementary admittance $Y_{\rm surf.} = [b/r]\mathrm{d}s$ which is smaller than the "local access admittance" of order b/ρ. This "local access admittance" represents the admittance of the small bulk area which is in front of this part of the interface. The value of this local access admittance does not depend on the diameter of this area since the admittance of a square of electrolyte with thickness b is equal to $Y_{\rm acc.} = b/\rho$ whatever its size.

One can then consider a larger region between curvilinear abscissa s_1 and s_2. Depending on s_1 and s_2, there exist two situations: if the curvilinear distance between s_1 and s_2 is small, the current is limited by the surface impedance. Such an element works then uniformly. On the contrary, if this distance is large enough, the current is limited by the bulk resistance to access the surface, and such an object does not work uniformly. But in the latter situation, we are, in a first approximation, back in the case of a pure Laplacian field with the boundary condition $V = 0$, since it is the access to the surface that limits the current. Direct visual observation of the active region in irregular electrodes has shown that these facts are verified experimentally [20].

The idea then consists in coarse-graining locally the real geometry to a scale such that the perimeter $L_{\rm p1}$ in a region of size (or diameter) $L_{\rm c1}$ is given by the condition that the integral of $[b/r]\mathrm{d}s$ along that part of the perimeter is equal to the access admittance $Y_{\rm acc.} = b/\rho$. Equivalently, the integral of $\mathrm{d}s/\Lambda$ over that same region should be equal to 1. This means that the curvilinear distance $(s_2 - s_1)$ along the electrode is equal to Λ. The chord length $L_{\rm c}(s)$ is thus defined as the distance between s_1 and s_2 in real space. Practically, we use instead the "local" chord between the curvilinear coordinates $s_1 = s - \Lambda/2$ and $s_2 = s + \Lambda/2$.

Because of its definition, a coarse-grained region can be considered as working uniformly. At the same time, in the new coarse-grained geometry, we are dealing with a pure Dirichlet Laplacian field. We then shift from the real geometry to the coarse-grained geometry which is made of successive chords $L_{\rm c1} = L_{\rm c}(s_0, s_1)$, $L_{\rm c2} = L_{\rm c}(s_1, s_2)$, ... This coarse-graining process is illustrated in Figure 1b.

This operation can be performed whatever the value of Λ if no deep pores are present in the structure. We first consider this simple case where the structure conserves aspect ratios of order one at all scales – the other case will be discussed later. The curvilinear coordinate in the coarse-grained geometry is named s', as indicated in Figure 1b. The perimeter of the coarse-grained electrode is named $L_{p'}$. Each element or grain of the coarse-grained system presents an admittance b/ρ, so that the differential admittance of an element $\mathrm{d}s'$ is equal to $[b/\rho L_{\rm c}(s')]\mathrm{d}s'$. By definition of the coarse-graining, the coarse-grained electrode works under Dirichlet boundary conditions. If there were no screening, the total coarse-grained electrode would be working uniformly and its admittance would be

$$Y_{\rm cg,noscreening} = \int_{\rm cg} \frac{b}{\rho L_{\rm c}(s')}\, \mathrm{d}s', \tag{11}$$

where the integral is taken along the coarse-grained geometry. But due to electric screening, there exists an active

zone where most of the current arrives and a passive zone which receives only little current [11], so that the integral can be split in:

$$Y_{\rm cg,noscreening} = \int_{\rm cg,act.} \frac{b}{\rho L_{\rm c}(s')}\ {\rm d}s' + \int_{\rm cg,pass.} \frac{b}{\rho L_{\rm c}(s')}\ {\rm d}s'. \tag{12}$$

The electrode admittance $Y_{\rm ode}$ is simply the first integral above. If one calls $L_{\rm act.cg}$ the length of the active zone of the coarse-grained electrode, this integral can be written

$$Y_{\rm ode} = L_{\rm act.cg}\ \frac{b}{\rho} \int_{\rm cg,act.} \frac{1}{L_{\rm c}(s')}\ \frac{{\rm d}s'}{L_{\rm act.cg}}\cdot \tag{13}$$

The integral represents the inverse harmonic mean of $L_c(s')$ along the active zone. This average is called $\langle L_c\rangle_{\rm act.}$:

$$\langle L_c\rangle_{\rm act.}^{-1} = \frac{1}{L_{\rm act.cg}} \int_{\rm cg,act.} \frac{{\rm d}s'}{L_{\rm c}(s')}\cdot \tag{14}$$

Our essential hypothesis, using a simplistic interpretation of Makarov's theorem, is that the active zone has a size $L_{\rm act.cg}$ of the order of the electrode size L. The admittance then takes the very simple expression

$$Y_{\rm ode} = \frac{b}{\rho}\ \frac{L}{\langle L_{\rm c}\rangle_{\rm act.}}\cdot \tag{15}$$

The fact that $L_{\rm act.cg}$ is not exactly equal to L will be discussed later. At this stage the problem has been simplified without any loss of generality but still requires finding the active zone of the coarse-grained electrode in order to compute $\langle L_{\rm c}\rangle_{\rm act.}$ from equation (8). One can go one step further for the wide variety of systems for which one can approximate the harmonic mean on the active zone of the coarse-grained electrode by the value of the harmonic mean on the entire electrode, namely

$$\langle L_{\rm c}\rangle_{\rm act.}^{-1} \approx \langle L_{\rm c}\rangle^{-1} = \frac{1}{L'_{\rm p}} \int_{\rm cg} \frac{{\rm d}s'}{L_{\rm c}(s')}\cdot \tag{16}$$

Due to the fact that the harmonic mean is dominated by the small values of $L_{\rm c}(s')$, this approximation is valid unless the smallest values of the chord length $L_{\rm c}(s')$ are found only in the non-active region of the electrode. A counter-example to equation (16) could then be the special case of deep fjords with narrow access channels and small values of $L_{\rm c}$ only at the bottom of the fjords (note however that equations (7-9) are still valid in this case).

Apart from these cases, the harmonic mean of the chord length will be the same if taken along the active zone or along the total coarse-grained structure, and the admittance is

$$Y_{\rm ode} = \frac{b}{\rho}\ \frac{L}{\langle L_{\rm c}\rangle}\cdot \tag{17}$$

A very simple result is then achieved: the impedance of an irregular electrode in $d = 2$ is simply the square impedance ρ/b of the electrolyte divided by the number of chords needed to measure the size (or diameter) L of the electrode. This apparently simple result is not trivial. It expresses how the resistance of the electrode depends on the *electrolyte resistivity* and an average chord length corresponding to a perimeter of length Λ. The geometry enters through the relation between a perimeter of length Λ and its associated chord.

As there exists an exact mapping between s and s' with ${\rm d}s/\Lambda = {\rm d}s'/L_{\rm c}(s')$, the average chord length can be written also, working on the initial non coarse-grained geometry

$$\langle L_{\rm c}\rangle^{-1} \ = \ \frac{1}{L'_{\rm p}} \int_{\rm electrode} \frac{{\rm d}s}{\Lambda} \tag{18}$$

and using

$$L'_{\rm p} \ = \ \int_{\rm cg} {\rm d}s' \ = \ \int_{\rm electrode} \frac{L_{\rm c}(s)}{\Lambda}\ {\rm d}s \tag{19}$$

we find

$$\langle L_{\rm c}\rangle \ = \ \frac{1}{L} \int_{\rm electrode} L_{\rm c}(s)\ {\rm d}s. \tag{20}$$

As a consequence, it is equivalent to consider the harmonic mean of $L_{\rm c}$ on the coarse-grained electrode or the arithmetic mean on the real electrode. Note that equation (20) can be written

$$\langle L_{\rm c}\rangle \ = \ \frac{\Lambda}{\langle S(s)\rangle_{\rm H}}, \tag{21}$$

where

$$\frac{1}{\langle S(s)\rangle_{\rm H}} \ = \ \frac{1}{L} \int_{\rm electrode} \frac{L_{\rm c}(s)}{\Lambda}\ {\rm d}s. \tag{22}$$

The quantity $\langle S(s)\rangle_{\rm H}$ is the harmonic mean over the electrode of a "local" Dirichlet screening factor $S(s) = \Lambda/L_{\rm c}(s)$. In that sense $\langle L_{\rm c}\rangle$ measures the average screening on a perimeter scale Λ.

In the case where narrow pores are present in the structure, the coarse-graining cannot be performed, because above some size, the access to the surface can no more be a square of electrolyte but is a narrow conductor with an access resistance larger than ρ/b. However, the active zone is still well defined by equation (7) and can be measured through equation (9).

The electrode response is related to the chord associated to Λ. It exists then *three* regimes, depending on the value of Λ compared with the smaller cut-off length l and the total perimeter $L_{\rm p}$ of the working electrode. The three regimes correspond respectively to $\Lambda \ll l$, $l < \Lambda < L_{\rm p}$ and $L_{\rm p} \ll \Lambda$. The intermediate regime (secondary current distribution in electrochemistry) for which $l < \Lambda < L_{\rm p}$ can be very wide for a porous or fractal electrode. Between these regimes, there should exist crossovers around $\Lambda = l$ and $\Lambda = L_{\rm p}$.

When $\Lambda = r/\rho$ is much larger than L_p, that is in the case of a very resistive or strongly polarizable electrode, the current is uniform and trivially

$$Z_\mathrm{ode} = \frac{r}{bL_\mathrm{p}} \cdot \tag{23}$$

This value is found with good precision in the numerical simulations that will be described later. Note that in this regime, $L_\mathrm{c} = L(\Lambda/L_\mathrm{p})$ and equation (23) can be written as $Z_\mathrm{ode} = (r/b)(L_\mathrm{c}/L\Lambda) = (\rho/b)(L_\mathrm{c}/L)$, which means that equation (17) still applies in this regime. The impedance being proportional to r, the spectroscopic and heat impedance are strictly equal, due to equation (9). As a consequence, the length of the active zone calculated from the spectroscopic impedance should be exactly equal to the value given by equation (7). For the trivial regime where $j_\mathrm{n,N} = 1/L_\mathrm{p}$, one finds (using Eq. (7)) that $L_\mathrm{act.} = L_\mathrm{p}$, corresponding to equation (23).

4 The Makarov regime

For $\Lambda = (r/\rho) \ll l$, the chord L_c is equal to Λ, and equation (17) predicts

$$Z_\mathrm{ode} = \frac{r}{bL} \cdot \tag{24}$$

We call this regime the Makarov regime, because the distribution of the electric field is very close to that corresponding to Dirichlet boundary conditions in which $r = 0$. It corresponds to the primary current distribution in electrochemistry or to the response of a weakly polarizable electrode. Equation (24) can be called the "naive" prediction because it uses a very simplistic interpretation of Makarov result, namely that the length of the active zone is equal to L, whereas the correct statement would be that the length of the active zone should only be proportional to L.

Here again, the impedance is proportional to r, and the spectroscopic and heat impedance are strictly equal. The spectroscopic calculation gives an apparent size $L_\mathrm{app.}$ defined by

$$L_\mathrm{app.,spect.} = \lim_{r\to 0} \frac{r}{bZ_\mathrm{ode,spect.}} \cdot \tag{25}$$

It should be equal to $L_\mathrm{act.,heat}$ defined by equation(7) using the Dirichlet current distribution.

For a *given* electrode geometry, the apparent diameter $L_\mathrm{app.}$ is proportional to the size L of the electrode for any finite geometry. This can be justified by applying a dilatation transformation $x \to \Gamma x$ to all lengths. In that transformation, $j_\mathrm{n,N}(\Gamma x)$ becomes $j_\mathrm{n,N}(x)/\Gamma$ from the normalization condition. Then from equation (7), $L_\mathrm{act.,heat}$ transforms into $\Gamma L_\mathrm{act.,heat}$. In other words, $L_\mathrm{app.}$ really transforms like the size L of the electrode. The fact that $L_\mathrm{app.}$ is proportional but not equal to L is due to the fact that the current reaching the active zone is not uniformly distributed over this zone, as postulated in the Land Surveyor approximation.

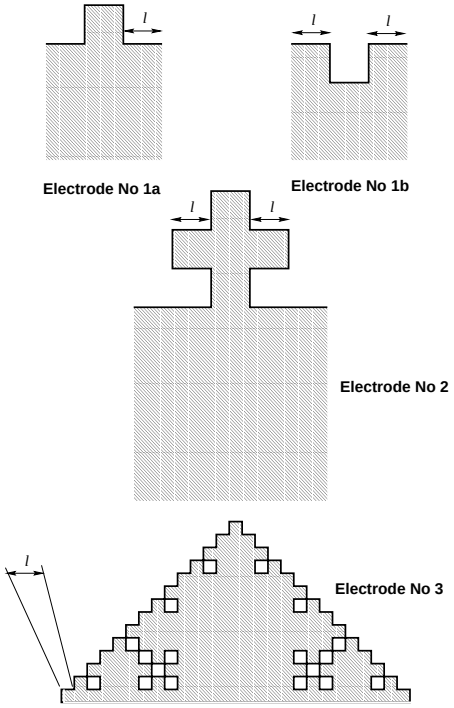

Fig. 2. Examples of electrode geometries under study. The smaller flat element has a length l. The geometry 1a is concave, while the geometry 1b is convex. The electrode No 3 is the third generation of the Vicsek electrode. The numerical results shown later have been computed with the fifth generation.

The Makarov regime has been studied numerically with some detail for the electrode shown in Figure 1a, using a finite difference method. The impedance is calculated using a square lattice discretization of space. The electrode surface is represented by resistances r in series with bulk resistances ρ, and we treat the corners as in reference [21]. In our computation, we use $\rho = 1$ and $b = 1$, so that the numerical parameter which measures the length Λ equals r. For the numerical solution of the Laplace equation, one uses over-relaxation with the constraint of exact current conservation and periodic boundary conditions. We have tested several convergence criteria. The electrode impedance $Z_\mathrm{ode,spec.}$ is obtained by $Z_\mathrm{ode,spec.} = Z_\mathrm{cell}(r) - Z_\mathrm{cell}(r = 0)$.

The results are given in Figure 3 to 5. In Figure 3, the impedance is found to be proportional to r with great precision. From the slope of Figure 3, one can compute the apparent spectroscopic length $L_\mathrm{app.}$ from equation (25). This length is different from the size $L = 3$. This is due to the non-uniform distribution of the current. As the current density exhibits a singularity around the salient corners, there is a dependence on the discretization parameter $\mathcal{N}$. This is shown in Figure 4, which gives the relative variation of the apparent length $(L_\mathrm{app.,spect.} - L)/L$ as a function of $\mathcal{N}$. The variation gives the effect of the discretization on the value of $L_\mathrm{app.,spec.}$. Above $\mathcal{N}$ of order 100, the effect of the discretization is weak.

The equality between $L_\mathrm{app.,spec.}$ and $L_\mathrm{app.,heat}$ can be verified numerically as, equation (7) in discretized form

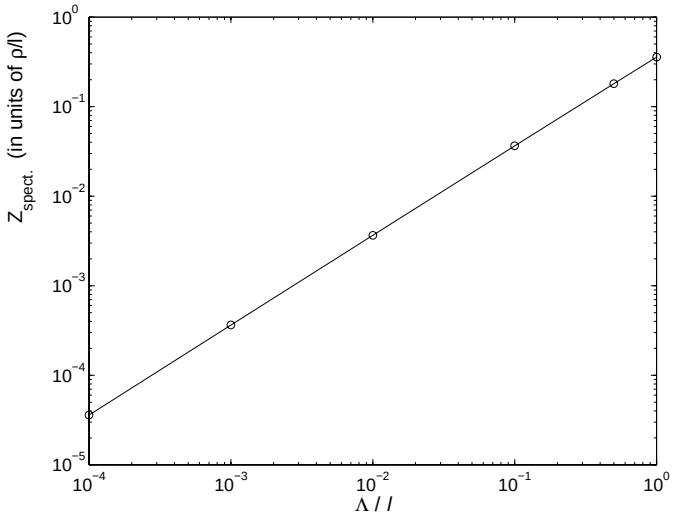

Fig. 3. Makarov response of electrode 1a computed with $N = 40$ segments along the size l. The slope of the curve gives the apparent length $L_{\mathrm{app.}}$ from equation (25).

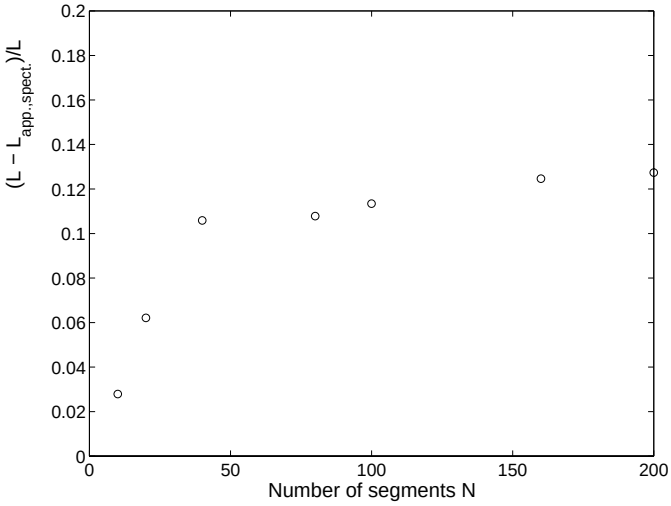

Fig. 4. Effect of the discretization on the value of the apparent length. Values of $(L-L_{\mathrm{app.}})/L$. The apparent length is deduced from plots as in Figure 3.

should read

$$L_{\mathrm{act.,heat}} = a \left(\sum_m j_m^2 \right)^{-1} , \qquad (26)$$

where the index m describes the various discretized sites of the working electrode and $a = 1/\mathcal{N}$ is the finite difference mesh spacing in the discretized Laplacian problem. As shown in the following paper, the equality between $L_{\mathrm{app.,spec.}}$ and $L_{\mathrm{app.,heat}}$ is exact even in the discretized version. The comparison between these two lengths is shown in Figure 5. The very good agreement between the values validates both the theory and the precision of the numerical investigation.

The result (26) can be used, together with the coarse-graining hypothesis, to obtain the impedance of a self-similar fractal electrode. Equation (7) indicates that $L_{\mathrm{app.}}$ scales like L^{D_2} when the size is increased keeping l constant (such an operation is not a dilation operation since the shape is modified). The exponent D_2 is named the correlation dimension of the harmonic measure, here the normalized current [22]. As the apparent size is a length, it has to be written $L_{\mathrm{app.}} = \mathrm{const.} L^{D_2}\ l^{1-D_2} = \mathrm{const.} L\ (l/L)^{1-D_2}$ because the only other length in the problem is l. Note that in a dilation operation where the shape is conserved $L_{\mathrm{app.}}$ is indeed proportional to L.

This result can be applied to the coarse-grained electrode, which works in the Makarov regime. Following equation (25), its impedance is

$$Z_{\mathrm{ode}} = \frac{r'_{\mathrm{cg}}}{b L_{\mathrm{app.cg}}} , \qquad (27)$$

where $L_{\mathrm{app.cg}} = \mathrm{const.} L^{D_2} L_{\mathrm{c}}^{(1-D_2)}$ and $r'_{\mathrm{cg}}/bL_{\mathrm{c}} = \rho/b$ or $r'_{\mathrm{cg}} = L_{\mathrm{c}}\rho$. The impedance can thus also be written

$$Z_{\mathrm{ode}} = \frac{1}{\mathrm{const.}} \frac{\rho}{b} \left(\frac{L_{\mathrm{c}}}{L} \right)^{D_2} . \qquad (28)$$

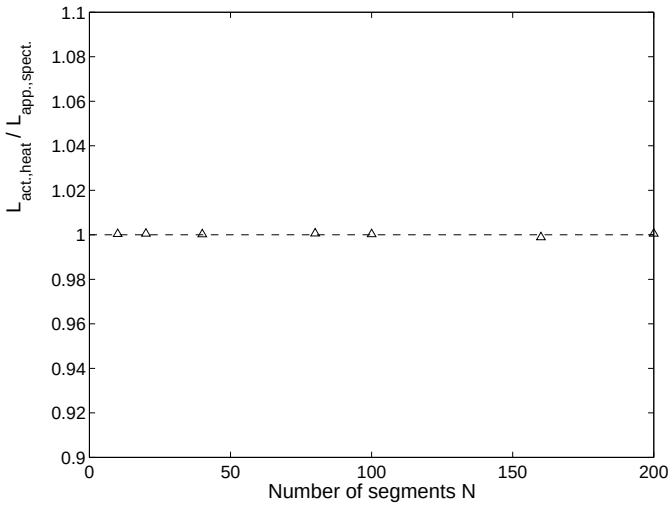

Fig. 5. Ratio of the length of the dissipative zone deduced from the integral of the square of the normalized current density (Eq. (7)) to the length of the active zone deduced from the measurement of the electrode impedance through equation (25) as a function of the discretization number $\mathcal{N}$.

For a self-similar fractal of dimension D_{f}, the chord length takes the very simple expression $L_{\mathrm{c}} = l\ (\Lambda/l)^{\frac{1}{D_{\mathrm{f}}}}$ and finally

$$Z_{\mathrm{ode}} = \frac{1}{\mathrm{const.}} \frac{\rho}{b} \left(\frac{1}{L} \right)^{D_2} l^{D_2\left(\frac{D_{\mathrm{f}}-1}{D_{\mathrm{f}}}\right)} \left(\frac{r}{\rho} \right)^{\frac{D_2}{D_{\mathrm{f}}}} . \qquad (29)$$

The role of D_2 was first stressed by Leibig and Halsey [23], Ball [24] and Ruiz-Estrada *et al.* [25]. This exponent D_2 being close to 1 even for very irregular electrodes, the approximation $L_{\mathrm{app.}} \approx L$ is always a good approximation.

5 Numerical study of the Land Surveyor approximation

In the following, the values of the different impedances ($Z_{\mathrm{ode,spect.}}(r)$ given by equation (2), $Z_{\mathrm{ode,heat}}(r)$ given by Eq. (7) and the same quantity using the land surveyor Eq. (17)) are computed numerically for the irregular electrodes of Figure 2. From here and below, the impedances and the current distributions are calculated using a finite element method. This method allows the study of very irregular and fractal electrodes, as a critical test of the quality of our approximations. For this, we need to study geometries where the ratio L/l is very large. The study of the Makarov regime for these electrodes would need to be of the order of 100 sites on the smaller feature l to be able to reach the continuous limit. The total linear size of the mesh would then be of order $100(L/l) \times 100(L/l)$, a very large number, making computations extremely long. On the other hand, the Makarov regime can be thought to be explained both by the theory and verified by the previous numerics. Moreover, the Makarov regime is interesting from a theoretical point of view, but it is a regime in which the impedance of the electrode is very small as compared with the impedance to access the electrode, and in consequence, the total flux is limited by the access resistance. Practical exchanger systems will work far from the Makarov regime. For all these reasons, the numerical study has been made using finite elements and a meshing which is not sufficient to study the Makarov regime with precision but sufficient to study the other regimes.

A finite element method is used with $l = 1$ and $\rho = 1$. The standard variational formulation of the problem is discretized with a triangular mesh and P_1-Lagrange interpolation. The linear system obtained in such a way is solved by using the Cholesky method, from the Finite Element Library MODULEF (*cf.* Bernadou *et al.* [26]). Examples of meshing are shown in Figure 6.

The results for electrode 1a, 2 and 3 are given in Figure 7. In this figure, and for each of the electrodes, the curve, the triangles, and the circles give respectively the land surveyor prediction, the spectroscopic impedance, and the heat impedance computed from the distribution of the normalized current densities through equation (7). One observes the existence of the three regimes corresponding respectively to $\Lambda \ll l$, $l < \Lambda < L_{\mathrm{p}}$, and $\Lambda \gg L_{\mathrm{p}}$. The general agreement between the different impedances and the land surveyor approximation can be considered satisfactory.

Note however that the logarithmic scale which is necessary to present the global behavior in Figure 7 may hide local discrepancies. To check more accurately these discrepancies, the ratio Λ/Z_{ode} (or r/Z_{ode} in computer units) is plotted in Figure 8. One can observe more clearly the deviations between the results. The maximum deviation for all three electrodes over the entire frequency range is of the order of 20%. For electrode 1 and 2, the deviations observed for small Λ is due to the fact that $L_{\mathrm{app.}}$ is slightly different from the diameter L. The numerical values of Λ/Z_{ode} for small Λ ($\Lambda \langle l$) should not be considered good for electrode No 3 because of the insufficient numerical meshing of the smaller cutoff of the fractal geometry.

The linear regime for large Λ is found with an extremely good precision in all three cases. In computer units, the prediction for Λ/Z_{ode} is L_{p}, that is respectively 5, 15, and 3125 for the curves 1a, 2, and 3 of Figure 8, corresponding to the three electrodes.

One can observe that the agreement between the land surveyor approximation (the continuous line) and the heat impedance (the circles) is better than with the spectroscopic impedance. This is due to the fact that this approximation is really an approximation of the length of the active zone. One should also note that the land surveyor method gives naturally the crossover regimes, which are generally out of scope of the theories which deal separately with one of the three regimes which really exist.

At last, a restrictive remark should be expressed: the geometrical evaluation of the chords lengths does not depend on the accessibility of the electrode. In other words, the method predicts the same impedance for a concave geometry, like in electrode 1a, and for a convex geometry like in the case of electrode 1b. But the real behavior is slightly different, as shown in Figure 9. This indicates a limitation of the method.

6 The inverse problem: can one hear the shape of an electrode?

Due to the good agreement between the land surveyor method, based on the electrode topography only, and the (supposedly) exact numerical values, one can examine the inverse problem. This inverse problem can be stated in the following manner: If one is able to measure the electrode impedance with infinite precision, is it possible to retrieve its geometry, or some geometrical characteristics of its geometry, from the impedance data? By measuring the impedance one would measure $Z_{\mathrm{ode,spec.}}$ as a function of the faradaic resistance r.

Of course, this is not possible practically, because r describes the rate of the electrochemical process at the interface. It is not an adjustable parameter in a real electrochemical experiment. By the impedance we mean impedance spectroscopy as function of frequency, but this will be discussed later [29]. Here, we consider only the dependence of the impedance as a function of r, as if r could be varied from 0 to infinity.

The inverse problem can be formulated in two steps. The first step is: can one hear the length of the active zone? The second question is: can one hear the shape? To answer the first question, we have studied, in addition to the previous electrodes, the response of the porous electrodes shown in Figure 10. The geometry of electrode No 4 presents a deep irregular pore, the electrode No 5 presents a narrow entry, and the electrode No 6 corresponds to a disconnected geometry kept at uniform potential. The length of the active zone is computed with the use of equation (9), and it is compared to the length of the active zone obtained directly from equation (7).

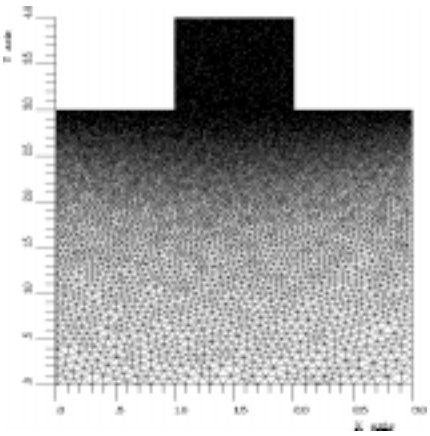

Electrode No 1a

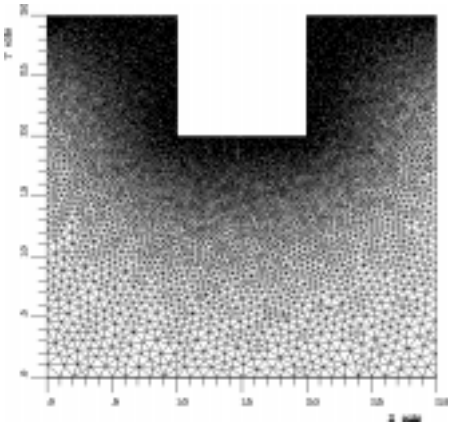

Electrode No 1b

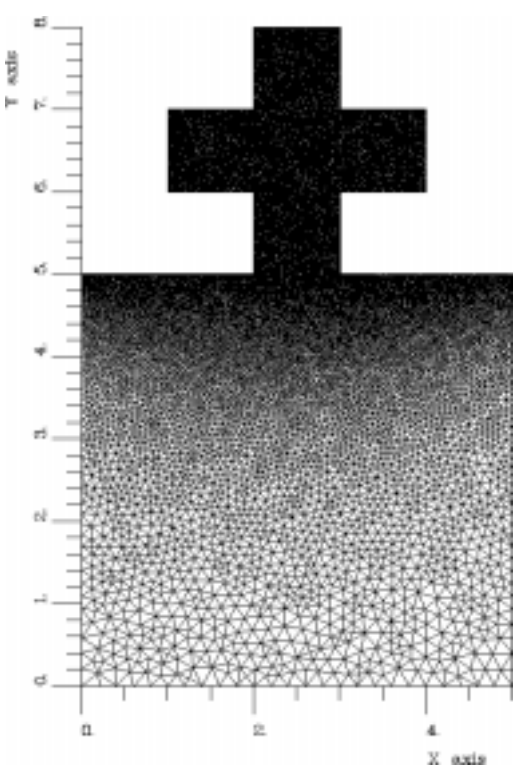

Electrode No 2

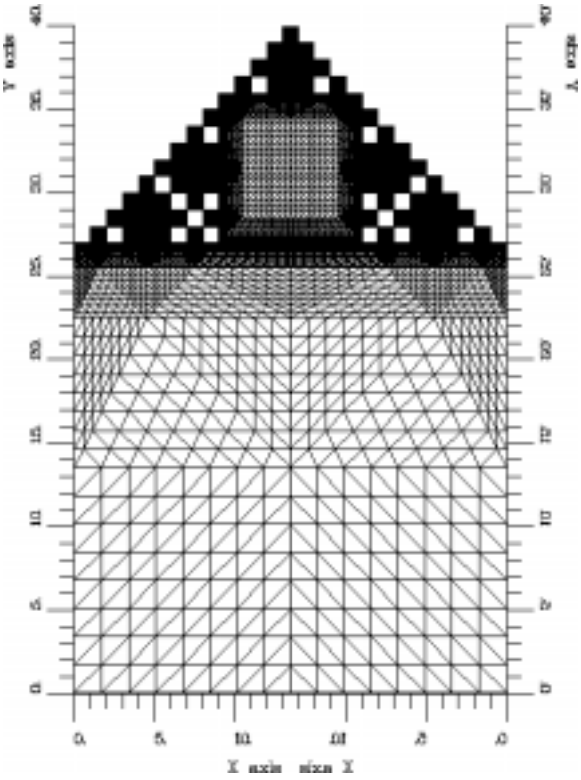

Electrode No 3

Fig. 6. Examples of finite element meshing. Note the fractal deterministic meshing used for the study of electrode 3.

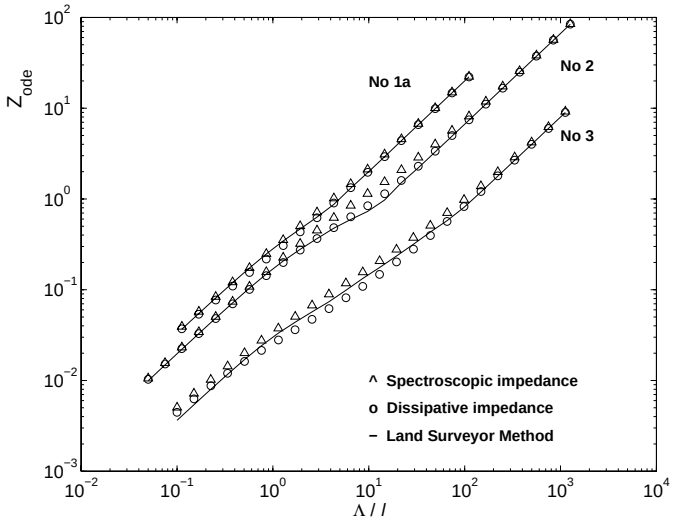

Fig. 7. Comparison between the land surveyor method and numerical values of $Z_{\mathrm{ode,spec.}}$ and $Z_{\mathrm{ode,heat}}$. The curve, the triangles, and the circles give respectively the land surveyor prediction, the spectroscopic impedance, and the heat impedance computed from the distribution of the normalized current densities through equation (7). One can distinguish between three regimes (Makarov's regime where $\Lambda \ll l$, the intermediate regime where $l < \Lambda < L_{\mathrm{p}}$, and the purely ohmic regime where $L_{\mathrm{p}} \ll \Lambda$), linked by two crossovers, around $\Lambda = l$ and around $\Lambda = L_{\mathrm{p}}$. For electrode 1a, $L = 3$ and $L_{\mathrm{p}} = 5$, for electrode 2, $L = 5$ and $L_{\mathrm{p}} = 15$, and for electrode 3 studied in the generation 5 of fractal iteration $L = 243$ and $L_{\mathrm{p}} = 3125$.

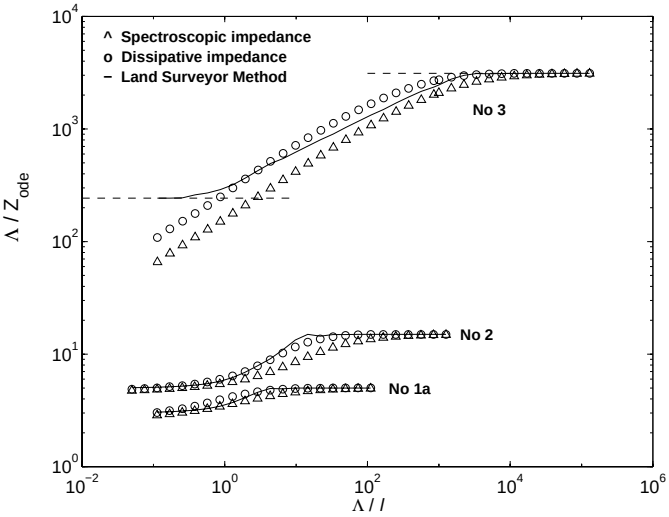

Fig. 8. Ratio Λ/Z_{ode} as a function of Λ for electrodes No 1a, 2 and 3. Note that this ratio is an estimate of the active length of the electrode. The dashed horizontal lines for electrode No 3 indicates the values of the size $L = 243$ and the perimeter $L_{\mathrm{p}} = 3125$.

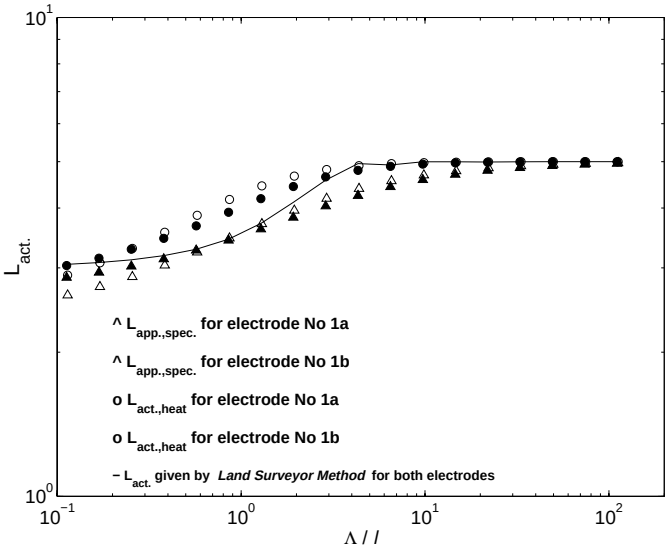

Fig. 9. Comparison between the response of concave (1a) and convex (1b) electrodes with the same geometry.

The results are shown in Figure 11 for all six geometries. The agreement is excellent. In consequence, one can always consider that impedance spectroscopy gives, using equation (9) to compute the heat impedance, a direct measurement of the length of the active zone as defined physically from the heat impedance. Note that the direct use of the spectroscopic impedance, indicated by the crosses in Figure 11, gives only an approximate value of $L_{\mathrm{act.heat}}$.

The second question is: can one hear the shape? Considering the inverse problem means that we work in a blind manner and measure directly an "electrochemical" chord length $L_{\mathrm{c,electr.}}(\Lambda)$ from equation (17). In computer units (ρ and $b = 1$) we compute

$$L_{\mathrm{c,electr.}}(\Lambda) = L.Z_{\mathrm{ode,heat}}(\Lambda). \tag{30}$$

$L_{\mathrm{c,electr.}}(\Lambda)$ then is the quantity that can be measured through impedance spectroscopy using equation (9). This length, which depends on geometry and Λ, can be compared to the direct determination obtained from the geometry through the use of relation (20).

The results are shown in Figure 12. The general agreement is good for electrodes No 1a, 2, 3 and 4 and only partial for the electrode No 5 presenting a narrow pore entry. (In the case of the disconnected electrode No 6 we have no means to implement the LS method.) We thus have a method which gives a direct measurement of the chord length with good accuracy for irregular geometries when the aspect ratio of the pores is not too large. It is in that sense that impedance spectroscopy gives a mean to "measure" the shape. Really, what has been done above is to transform the physical problem in a purely mathematical question: Given a curve, is it possible to retrieve its shape from the variation of the average chord length between two points as a function of the curvilinear distance between these points? This constitutes the mathematical **problem I**.

One can also use impedance data to give a diagnostic of the existence of deep porosity, when one observes the intermediate and the resistive regime. In the high resistivity regime, the impedance (Eq. (23)) is equal to r/bL_{p}. Then, measuring Z_{ode} yields L_{p} and the value of the crossover which must be around $\Lambda = L_{\mathrm{p}}$. A major discrepancy between this theoretical crossover and the real data indicates the presence of a deep porosity in the electrode structure.

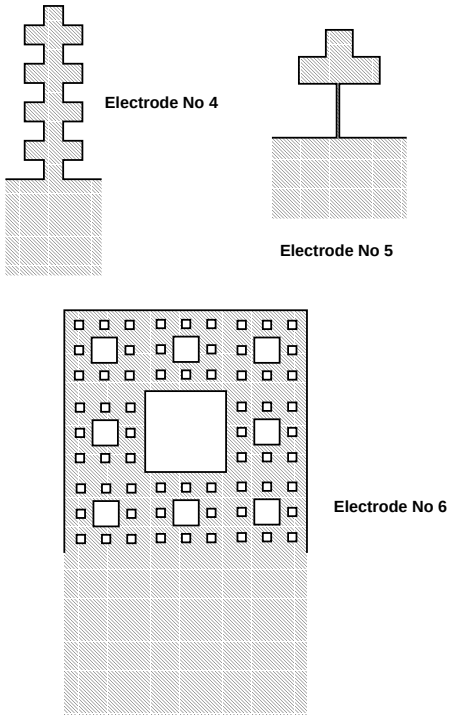

Fig. 10. Three porous electrodes.

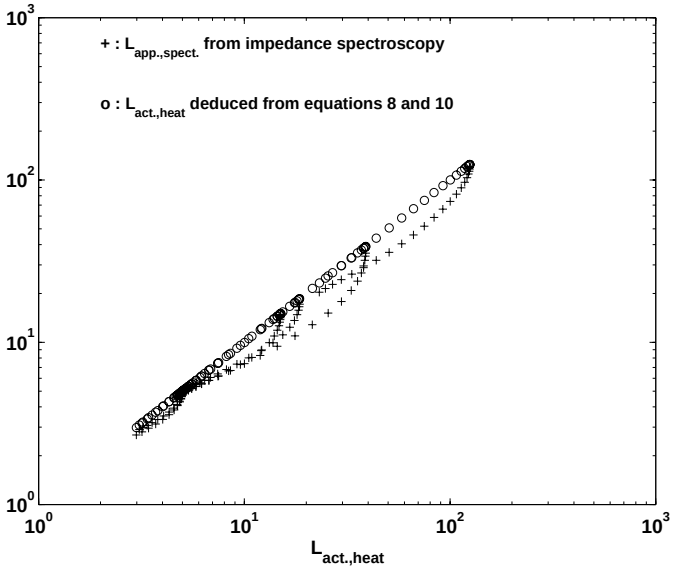

Fig. 11. Comparison between the length of the real active zone determined by the current distribution (Eq. 7), the length of the active zone deduced directly from the spectroscopic impedance (crosses) and the length of the active deduced from the spectroscopic impedance by the use of equations (8) and (9) (circles). The data corresponds to all six electrodes No 1 to 6 and for various values of Λ. One observes the identity relation predicted by the theory.

These conclusions are general. They apply to any linear Laplacian transport across a resistive interface. To be applied to real systems, the role of the counter electrode (or source) and the generalization to 3D situations should be examined.

7 Role of the counter-electrode and extension to 3D cells

The above results have been obtained under the assumption that the counter electrode is far enough from the working interface. In that situation, and except for the case of high resistivity of the interface, the effective transfer through the interface is limited by the access resistance R_0 of order ρ/b which is larger than the electrode impedance given by equation (17). If one is interested in increasing the current, one would set the counter-electrode closer to the working electrode, in order to minimize the global access resistance. The question arises then of the validity of the above results in the case of a close counter electrode. It will be shown now that the distance of the counter electrode has only a weak effect on the value of the electrode impedance. This is due to the fact that the equipotential lines are approximately flat even near the irregular interface region and this whatever the value of r. This is shown in Figure 13. It is qualitatively clear that the substitution of a near equipotential line, which is approximately flat, by a perfectly flat counter electrode will be of little effect. Moreover, the global transfer in that situation is given approximately by the interface impedance only as the impedance of the "cell" is of the same order as the impedance of the electrode, as indicated in Figure 13c.

Real electrochemical cells are generally 3d systems and the irregular electrodes are rough surfaces embedded in 3 dimensions. The above comparison has not yet been studied in 3d, but the partial theoretical and experimental results that we have for that case can be generalized simply. For that, one has to consider an element of surface of total area A which exhibits a surface impedance r/A. If the diameter of that surface element is L_A, the access resistance is of order ρ/L_A. The crossover which defines the size of the coarse graining is then obtained when $r/A_{\rm cg} = \rho/L_{\rm cg}$ or $A_{\rm cg}/L_{\rm cg} = r/\rho = \Lambda$. Note that a length A/L_A is of the order of the perimeter of a cut of the rough surface by a plane. This can be formulated in a precise manner for a fractal electrode [7].

The same type of discussion can be given for irregular surfaces in 3d. In the Makarov regime, the impedance takes the form

$$Z_{\rm ode,heat} = Z_{\rm ode,spect.} = \frac{r}{A_{\rm act.}} \tag{31}$$

with

$$A_{\rm act.} = \left[\int_{\rm electrode} j_{\rm n,N}^2 \, {\rm d}A\right]^{-1}. \tag{32}$$

The area of the active zone $A_{\rm act.}$ will be of the order of L^2, the square of the electrode diameter.

In the high resistivity regime, the impedance will take the form

$$Z_{\rm ode,heat} = Z_{\rm ode,spect.} = \frac{r}{A_{\rm p}}, \tag{33}$$

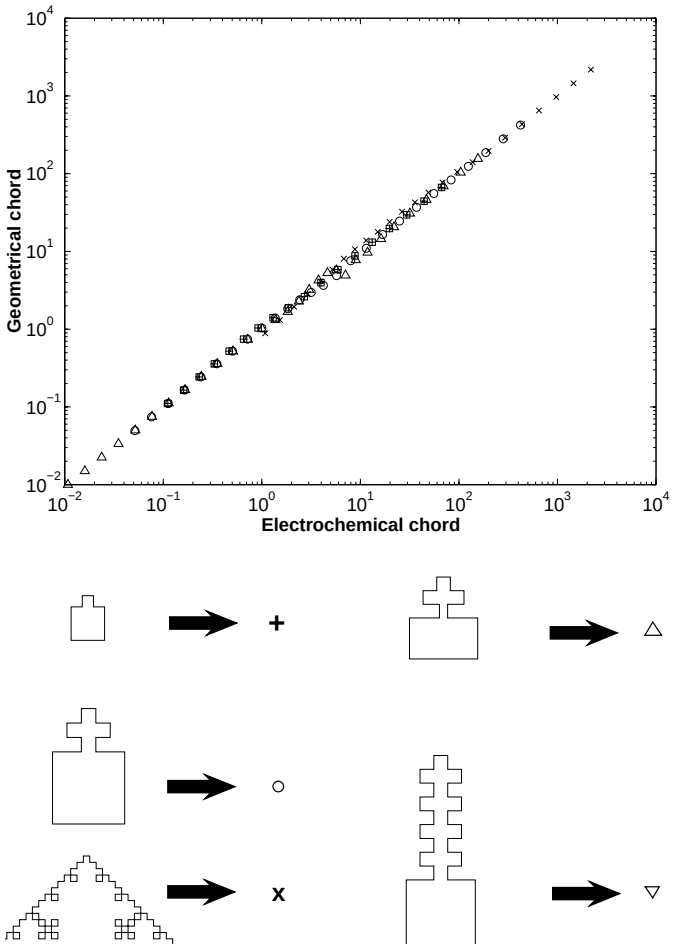

Fig. 12. Comparison between the "electrochemical" average chord $L_{\mathrm{c,electr.}}(\Lambda)$ given by equation (26) and the purely geometrical average chord $L_{\mathrm{c,geo.}}(\Lambda)$ deduced from equation (9) for electrodes No 1 to 5 and for various values of Λ.

where A_{p} is the total area of the electrode surface.

In the intermediate regime, the impedance Z_{ode} will be approximately equal to $[\rho/L_{\mathrm{cg}}(\Lambda)][L_{\mathrm{cg}}(\Lambda)/L]^2$ or

$$Z_{\mathrm{ode}} \approx \rho L_{\mathrm{g}}(\Lambda)/L^2, \tag{34}$$

where $L_{\mathrm{cg}}(\Lambda)$ is the diameter of a zone such that the perimeter of a cut of the rough surface by a plane is of order Λ. Equations implying the same type of approximation as (34) have been shown to apply approximately to the impedance spectroscopy of highly ramified blocking electrodes [28]. It should however be stressed that the validity of this expression has not been verified by extensive numerical simulation for various 3d geometries.

For self-similar fractal electrodes in 3d, the equations (31, 32) used in the coarse-grained electrodes should be written, following the same type of arguments developed in section 4 on the correlation dimension,

$$Z_{\mathrm{ode}} = \text{const. } \rho \left(\frac{1}{L}\right)^{D_2} l^{\frac{(D_2-1)(D_f-2)}{(D_f-1)}} \left(\frac{r}{\rho}\right)^{\frac{(D_2-1)}{(D_f-1)}}. \tag{35}$$

8 Impedance spectroscopy of irregular interfaces

Impedance "spectroscopy" means the measurement of the electrode impedance as a function of frequency and not as discussed above the measurement of the electrode impedance as a function of r or Λ. In a.c., the faradaic resistance r should be replaced by $1/(r^{-1} + j\gamma\omega)$, where γ is the specific admittance of the electrodic interface. Because the response of the system is linear and causal, the impedance is an analytic function of the frequency ω. Then, if one can predict the functional dependence of the impedance as a function of r, the response for arbitrary frequency will be obtained by substitution of r by $1/(r^{-1} + j\gamma\omega) = r/[1 + (r\gamma\omega)^2]^{1/2}.\exp(-j\gamma\omega r)$. Our method, however, does not provide directly the functional dependence as a function of frequency.

In the Makarov regime and resistive regime, the impedance will be respectively

$$Z_{\mathrm{ode}} = \frac{r}{\sqrt{1 + (r\gamma\omega)^2}} \frac{\exp(-j\gamma\omega r)}{bL_{\mathrm{act.}}} \tag{36}$$

and

$$Z_{\mathrm{ode}} = \frac{r}{\sqrt{1 + (r\gamma\omega)^2}} \frac{\exp(-j\gamma\omega r)}{bL_{\mathrm{p}}} \tag{37}$$

with corresponding expressions for surfaces in 3d. In the intermediate regime, the dependence on r is non-linear and the transposition is more delicate. From the graphs of Figure 7, one observes that, to a reasonable approximation, the dependence can be fitted by a power law. In that case, the a.c. response will be in first approximation a power law of the argument $r/[1 + (r\gamma\omega)^2]^{1/2} \exp(j\gamma\omega r)$. The modulus of this power law will be the same power law of the modulus $r/[1 + (r\gamma\omega)^2]^{1/2}$. The procedure is then to measure the modulus of the impedance as a function of frequency and to insert $r/[1 + (r\gamma\omega)^2]^{1/2}$ in the calculus of L_{c} from $\Lambda(\omega) = r/\rho[1 + (r\gamma\omega)^2]^{1/2}$. For a blocking electrode with $r = \infty$, one should substitute r by $(\gamma\omega)^{-1}$ everywhere in the above expressions, and $\Lambda = r/\rho$ should be replaced by $\Lambda = 1/\rho\gamma\omega$. Impedance spectroscopy will then provide some knowledge about the geometry when the length $\Lambda(\omega) = r/\rho[1 + (r\gamma\omega)^2]^{1/2}$ is of the order of the perimeters of the various geometrical irregularities. For values of the frequencies such that $r\gamma\omega\langle 1$, $\Lambda(\omega)$ will be of the order of $(r/\rho)[1 - (1/2)(r\gamma\omega)^{-2}]$ and will be roughly independent of frequency. In that situation, impedance spectroscopy will not provide a way to explore the geometry. On the opposite, if $r\gamma\omega\rangle 1$, $\Lambda(\omega)$ will be of the order of $1/\rho\gamma\omega$ and impedance spectroscopy provides a way to explore the geometry. In this situation, the equation (9) should be written

$$Z_{\mathrm{ode,heat}} = -\ \omega\ \frac{\partial Z_{\mathrm{ode,spect.}}}{\partial\omega} \tag{38}$$

and this value should be used to compute L_{c}.

The conclusion that we have obtained, namely the approximate measurement of the chord length, may also be

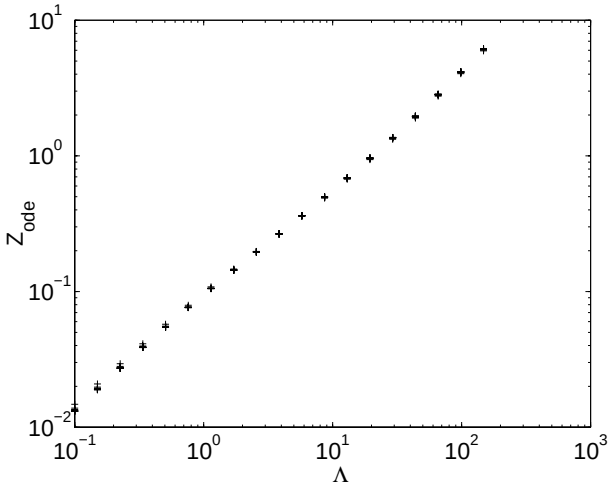

(a)

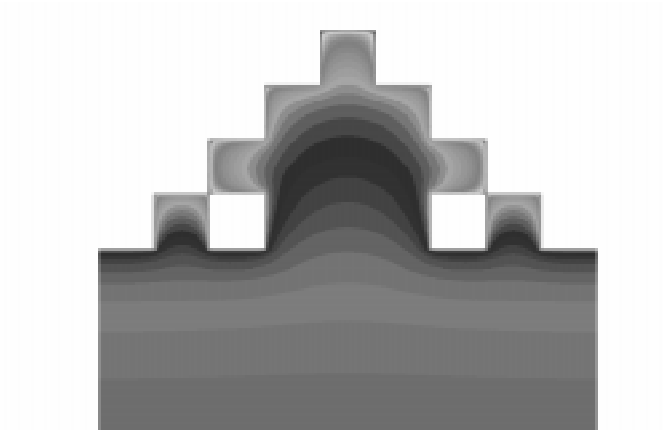

(b)

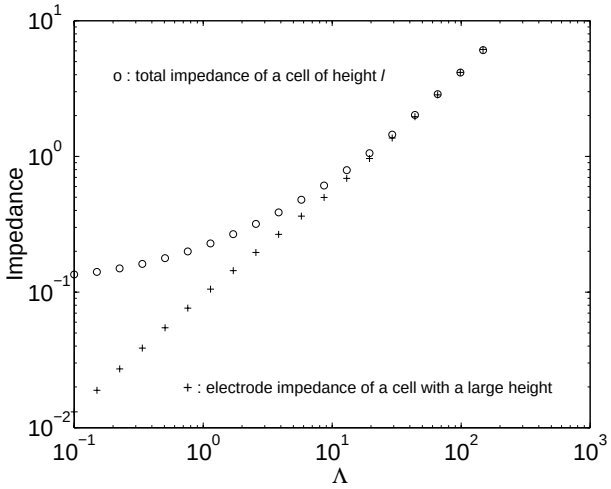

(c)

Fig. 13. Influence of the distance of the counter electrode for a working fractal electrode with $L = 9$. The electrode impedance $Z_{\rm ode}(\Lambda)$ is computed for 10 values of the counter electrode distance d, ranging from $d = L/10$ to $d = L$ (a). The dependence is found be very weak. This is due to the fact that the equipotential lines just outside the structure are nearly flat as shown in (b). (c) Comparison between the total cell impedance and the electrode impedance for $d = l$.

practically limited by the experimental accuracy in the impedance measurement. In a reverse way, the fact that the electrode impedance is expressed by such a simple expression as equation (17) is probably an important step to help to understand the contribution of a possible irregular geometry to the experimental results, as the impedance may be determined by other processes than the geometrical influence discussed here [6].

9 Applications to diffusional problems

An exactly equivalent problem is the steady state diffusion of neutral species towards an irregular interface (or membrane) in the same geometry [4]. This equivalence will be used extensively in the following theoretical paper. Here, the flux of a neutral species across a membrane is limited both by the diffusion from the source and the finite rate of transfer across the membrane. Instead of a counter electrode as in Figure 1, we imagine that some process maintains a constant concentration C_0 of the species of interest on a source situated in the same position as the counter electrode. In this system, the transport process can be described in terms of the vector flux $\boldsymbol{\Phi}$ at coordinate x. In the bulk diffusion obeys Fick's law, $\boldsymbol{\Phi} = -D\nabla C$, where C is the concentration of the particles of interest and D is the diffusion coefficient. The transfer across the membrane obeys the equation $\boldsymbol{\Phi}_{\rm n} = -WC$, where W is the probability per unit time, surface, and concentration for a particle to cross the membrane. In the last equation, we neglect

back transfer, supposing that the concentration on the other side of the membrane is maintained equal to zero. The conservation of the normal flux at the frontier can be written $C/\nabla_{\rm n}C = D/W = \Lambda$. In steady state, the concentration satisfies the stationary diffusion equation $\Delta C = 0$. These equations are equivalent to the current and potential equations, provided that we exchange $\boldsymbol{\Phi}$ for $\mathbf{J}$, $-\nabla C$ for $-\nabla V$, D for ρ^{-1} and W for r^{-1}. It is then possible to define a diffusion impedance $Z_{\rm D}$ by the relation between the total flux $\boldsymbol{\Phi}$ and the concentration $C_{\rm S}$ on the source $\boldsymbol{\Phi} = C_{\rm S}/Z_{\rm D}$. This diffusion impedance will obey the same law (17).

The diffusion equivalence helps to understand qualitatively why the behavior of a narrow entry pore is described with less precision by the land surveyor method described here. For finite Λ, a particle must collide several times before being absorbed. It that case, when a particle reaches a region near the entry of the pore, it will be absorbed not only near the point of arrival, but it has a fair chance to be absorbed on the other side of the pore entry. For this reason, our specific way to implement the coarse-graining effect gives a length which is smaller than it should be and the approximate Z is smaller that the real value. This is the cause of the discrepancy observed in Figure 12 for electrode No 5.

If one is looking for optimization of the transfer with fixed transport parameters, this optimization will be obtained when the surface of the irregular interface is working uniformly. This is obtained when the perimeter of a cut of the surface by a plane (of order A/L_A) is larger or equal to Λ. Consider for example the case of the chemical attack of a raw material. For example, an irregular solid is etched by G-molecules such that $G + \text{Solid} \rightarrow 0$ with a local reaction flux $\boldsymbol{\Phi} = -RC_G$, where R is the reactivity and C_G is the local concentration of G. In that case $\Lambda = D/R$. If $\Lambda \langle A/L_A$, the solid will not be attacked uniformly.

The same considerations should apply in the Eley-Rideal regime of heterogeneous catalysis. If a reaction $G \rightarrow G^*$ occurs on collision on an irregular pore wall with a finite probability, the local flux $\boldsymbol{\Phi}_{G^*}$ of creation of G^* at the surface is given by $\boldsymbol{\Phi}_{G^*} = -RC_G$, where R is the reactivity and C_G the local concentration of G. In the Eley- Rideal regime, the transport to the catalytic surface is limited by molecular diffusion. As above, the condition for the catalyst to work uniformly is that $A/L_A \leq \Lambda$, so that the catalyst grain should not be too large. The same considerations about optimization of the Laplacian transfer apply to the diffusion exchange of oxygen in the lung of mammals [5].

10 Conclusion

To sum up, we have developed a new method of computing the properties of electrochemical cells or equivalently the properties of rough absorbing interfaces *whatever their geometries in the various physical regimes, including the crossover regimes.*

We have tested a simple method to find the response of irregular electrodes in the linear response regime from their geometry alone. Apart from the interface geometry, all that is needed are the values of the microscopic transport coefficients. The robust character of this method makes it a good candidate for the study of the response of irregular electrodes in the non-linear regime, where the local current across the electrode is related to the local voltage by a non-linear relation $j = f(V)$.

The question addressed in the title can be answered in several steps. First, it has been verified numerically in $d = 2$ that impedance spectroscopy leads to the measure of the length of the active zone, whatever the geometry. The same result will be proved for any dimension in the following paper. Second, it provides a way to detect the existence of a deep porosity. It has been shown that, if no deep porosity exists, impedance spectroscopy measures approximately the average length of the chord associated with the perimeter length $\Lambda = (\rho\gamma\omega)^{-1}$. In this case, the physical question of determining the shape of the electrode from its impedance spectroscopy is transformed into a purely mathematical problem, called **problem I**:

"Given the average, over the electrode geometry, of the chord length $\langle L_{\rm c} \rangle$ associated to a parametric perimeter length Λ, can one retrieve the shape of the electrode?"

To our knowledge, the answer to this question is open.

The authors wish to acknowledge useful discussions with R. Ball, W. Dieterich, C. Evertz, Th. Halsey, P. Jones, M. Kolb, N. Makarov, B. Mandelbrot, J. Peyrière, P. Pfeifer and M. Rosso. This research was supported by N.A.T.O. grant C.R.G.900483. The Laboratoire de Physique de la Matière Condensée is "Unité Mixte de Recherches du Centre National de la Recherche Scientifique No. 7643".

References

1. M. Kac, Am. Math. Monthly **73**, 1 (1966).
2. C. Gordon, D. Webb, S. Wolpert, Bull. Am. Math. Soc. **27**, 134 (1992); S. Sridhar, A. Kudrolli, Phys. Rev. Lett. **72**, 2175 (1994).
3. M. Filoche, B. Sapoval, Eur. Phys. J. B **9**, 755 (1999).
4. B. Sapoval, Acta Stereolog. **6/III**, 785 (1987); J. Electrochem. Soc. **137**, 144C (1990); *Extended Abstracts, Spring Meeting of the Electrochemical Society, Montreal, Canada*, **90-1**, 772 (1990).
5. B. Sapoval, in *Fractals in biology and medicine*, edited by T.F. Nonnenmacher, G.A. Losa, E.R. Weibel (Birkhäuser-Verlag, Basel 1994), pp. 241-249.
6. T. Pajkossy, J. Electroanal. Chem. **300**, 1 (1991); Heterogeneous Chem. Rev. **2**, 143 (1995).
7. B. Sapoval, in *Fractals and disordered systems*, 2nd ed., edited by A. Bunde and S. Havlin (Springer-Verlag, 1996), pp. 232-261.
8. P. Pfeifer, B. Sapoval, Mat. Res. Soc. Symp. Proc. **366**, 271 (1995), M.R.S. Pittsburg.
9. M. Leibig, J. Phys. A: Math. Gen. **26**, 3349 (1993).
10. B. Sapoval, S. Russ, J.-P. Korb, D. Petit, Fractals **4**, 453 (1996).

11. B. Sapoval, Phys. Rev. Lett. **73**, 3314 (1994).
12. B. Duplantier, Phys. Rev. Lett. **66**, 1555 (1991).
13. L.I. Daikhin, A.A. Kornyshev, M. Urbakh, Phys. Rev. E **53**, 6192 (1996).
14. J.N. Agar, T.P. Hoar, Disc. Farad. Soc. **1**, 158 (1947); T.P. Hoar, J.N. Agar, Disc. Farad. Soc. **1**, 162 (1947).
15. C. Wagner, J. Electrochem. Soc. **98**, 116 (1951).
16. N.G. Makarov, Proc. London Math. Soc. **51**, 369 (1985).
17. P. Jones, T. Wolff, Acta Math. **161**, 131 (1988).
18. R.P. Wool, J.M. Long, Macromolec. **26**, 5227 (1993); R.P. Wool, *Structure and strength of polymer interfaces* (Hanser publ., 1994).
19. M. Filoche, B. Sapoval, J. Phys. I France **7**, 1487 (1997).
20. M. Rosso, Y. Huttel, E. Chassaing, B. Sapoval, R. Gutfraind, J. Electrochem. Soc. **144**, 1713 (1997).
21. R. Gutfraind, B. Sapoval, J. Phys. I France **3**, 1801 (1993).
22. see for example M. Schroeder, in *Fractals, Chaos, Power Laws* (W.H. Freeman, New York, 1991).
23. M. Leibig, T.C. Halsey, Electrochim. Acta, **38**, 1985 (1993) and references therein.
24. R.C. Ball, in *Surface Disordering, Growth, Roughening and Phase Transitions*, edited by R. Julien, J. Kertesz, P. Meakin, D. Wolf (Nova Science Publisher, 1993), p. 277.
25. H. Ruiz-Estrada, R. Blender, W. Dieterich, J. Phys.-Cond. Matter. **6**, 10509 (1994).
26. M. Bernadou *et al.*, *Modulef: une bibliothèque modulaire d'éléments finis* (INRIA, France, 1985).
27. B. Sapoval, R. Gutfraind, P. Meakin, M. Keddam, H. Takenouti, Phys. Rev. E **48**, 3333 (1993).
28. E. Chassaing, B. Sapoval, J. Electrochem. Soc. **141**, 2711 (1994).
29. see for example D.D. Macdonald, *Transient Techniques in Electrochemistry* (Plenum, New York, 1977); *Characterization of Electrodes and Electrochemical Processes* (The Electrochemical Society Series, John Wiley and Sons, New York, 1990) and references therein.